A Unified MPC Formulation for Control of Commercial HVAC Systems in Multiple Climate Zones

Naren Srivaths RAMAN^{1*}, Bo CHEN¹, Prabir BAROOAH¹

¹ University of Florida, Department of Mechanical and Aerospace Engineering, Gainesville, Florida, USA E-mail: narensraman@ufl.edu, bo.chen@ufl.edu, pbarooah@ufl.edu

* Corresponding Author

ABSTRACT

Model predictive control (MPC) has been widely investigated for climate control of commercial buildings for both energy efficiency and demand flexibility. However, most MPC formulations ignore humidity and latent heat. The inclusion of moisture makes the problem considerably more challenging, primarily since a cooling and dehumidifying coil model which accounts for both sensible and latent heat transfers is needed. In our recent work, we proposed an MPC controller in which humidity and latent heat were incorporated in a principled manner, by using a reduced-order model of the cooling coil. Because of the highly nonlinear nature of the process in a cooling coil, the model needs to be modified based on certain weather/climatic conditions to have sufficient prediction accuracy. Doing so, however, leads to a mixed-integer nonlinear program (MINLP) that is challenging to solve. In this work, we propose an MPC formulation that retains the NLP (nonlinear programming problem) structure in all climate zones/weather conditions. This feature makes the control system capable of autonomous operation. Simulations in multiple climate zones and weather conditions verify the energy savings performance, and autonomy of the proposed controller. We also compare the performance of the proposed MPC controller with an MPC formulation that does not explicitly consider humidity. Under certain conditions, it is found that the MPC controller that excludes humidity leads to poor humidity control, or higher energy usage as it is unaware of the latent load on the cooling coil.

1. INTRODUCTION

Model predictive control (MPC) for commercial heating, ventilation, and air conditioning (HVAC) systems for both energy efficiency and demand flexibility has been an active area of research (Serale et al., 2018; Shaikh et al., 2014). However, most MPC formulations ignore humidity and latent heat, focusing only on the sensible heat balance. The inclusion of moisture makes the problem considerably more challenging, primarily since a cooling and dehumidifying coil model which accounts for both sensible and latent heat transfers is needed. The heat transfer and condensation (moisture removal) process on the coil surface is a highly complex phenomenon. In addition to the challenge of modeling such a process, MPC requires that the model be simple. Since MPC uses the model as an equality constraint in an optimization problem that is solved in real-time, a complicated model will increase the computational complexity of the optimization problem.

In our recent work (Raman et al., 2020), we proposed an MPC controller in which humidity and latent heat were incorporated in a principled manner, by using a reduced order model of the cooling coil. However, such reduced order models might not work well when the operating conditions are extreme. Figure 1 shows the outdoor weather conditions for Miami, Florida and Tucson, Arizona. Miami has a hot and humid climate, while Tucson has a hot and dry climate. A possible method for handling such extreme climatic/weather conditions is to have multiple models, each designed to be valid for a specific operating condition. In the context of MPC, such model switching will lead to a mixed integer problem with integer valued variables deciding the model to be used for a particular time instant. Since each such model is nonlinear (especially for the cooling coil), the resulting problem will be an MINLP, and that too a high dimensional one especially if the planning horizon is long. Solving such high-dimensional MINLPs is significantly more challenging than NLPs (Kraemer & Marquardt, 2010).

In this paper, we propose an MPC formulation that can operate effectively in multiple climatic conditions that retains the NLP nature of the underlying optimization problem. The proposed MPC controller is called SL-MPC, where the

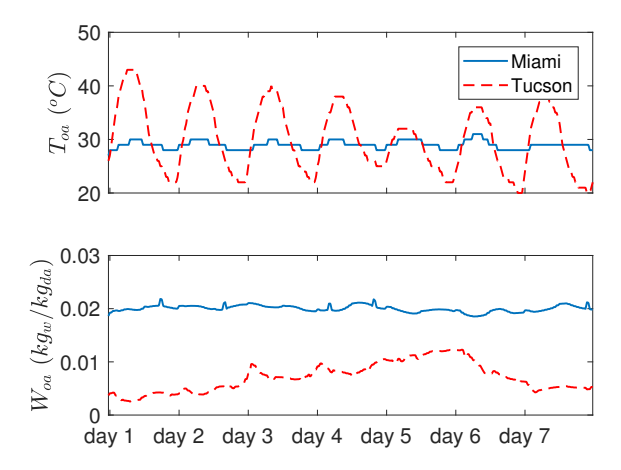


Figure 1: Outdoor weather comparison between Miami, Florida (hot-humid) and Tucson, Arizona (hot-dry) for a week during summer (July/25/2016 to July/31/2016 for Miami and June/06/2016 to June/12/2016 for Tucson). Data obtained from National Solar Radiation Database (nsrdb.nrel.gov). T_{oa} : outdoor air dry-bulb temperature, and W_{oa} : outdoor air humidity ratio.

prefix SL stands for "sensible and latent" heat. It uses the same data-driven model originally proposed in (Raman et al., 2020), and thus does not increase modeling complexity. The simple structure of the model—chosen to strike a compromise between prediction accuracy and simplicity needed for real-time optimization—puts a limit on its prediction in extreme conditions. The main innovation in the proposed formulation is that it uses additional slack variables, for water flow rates with additional constraints for some of the decision variables regarding the cooling and dehumidification coil. These modifications to the MPC formulation makes it climate/weather independent. Simulations in two extreme climate zones, from hot-dry to hot-humid, and multiple weather/seasonal conditions are reported that show the effectiveness of the proposed formulation in providing energy-efficient indoor climate control.

A secondary contribution of the paper is comparison of the proposed MPC scheme with two other control algorithms: (i) a rule-based "dual-maximum" controller as the baseline (ASHRAE, 2011), and (ii) a humidity-agnostic MPC formulation that we call S-MPC, with the prefix S standing for "sensible heat only". Simulations in the two climate zones show that the proposed controller provides more energy savings (over the baseline) than S-MPC. The S-MPC leads to violations in indoor humidity constraints in hot humid climates. More importantly, the proposed scheme is able to maintain temperature and humidity constraints in both climates and all weather conditions without requiring any climate or weather specific modifications in the formulation.

The rest of the paper is organized as follows. Section 2 describes the HVAC system considered in this work. Section 3 presents the proposed MPC-based control algorithm and the two other algorithms with which its performance is compared. The simulation setup is described in Section 4. Simulation results are presented and discussed in Section 5. Finally, the main conclusions are provided in Section 6.

2. SYSTEM DESCRIPTION

In this paper we consider a single-zone commercial variable-air-volume HVAC system, whose schematic is shown in Figure 2. In such a system, part of the air exhausted from the zone is recirculated and mixed with fresh outdoor air. If the mixed air is too cold, it is first heated at the preheating coil so that the downstream cooling coil is protected from freezing and the resulting damage. Then this mixed air is sent through the cooling coil where it is cooled and dehumidified to the conditioned air temperature (T_{ca}) and humidity ratio (W_{ca}). If the air before the cooling coil is dry, then there is only cooling but no dehumidification, i.e., $T_{ca} < T_{pha}$ and $W_{ca} = W_{pha}$, where T_{pha} and W_{pha} are the temperature and humidity ratio of air before the cooling coil respectively. The conditioned air is passed through the heating coil where it is heated to the supply air temperature (T_{sa}) and finally supplied to the zone. There is no water vapor phase change across the heating or preheating coils, so the humidity ratio of the supply air is the same as the conditioned air ($W_{sa} = W_{ca}$), and the humidity ratio of the preheated air is the same as the mixed air ($W_{pha} = W_{ma}$).

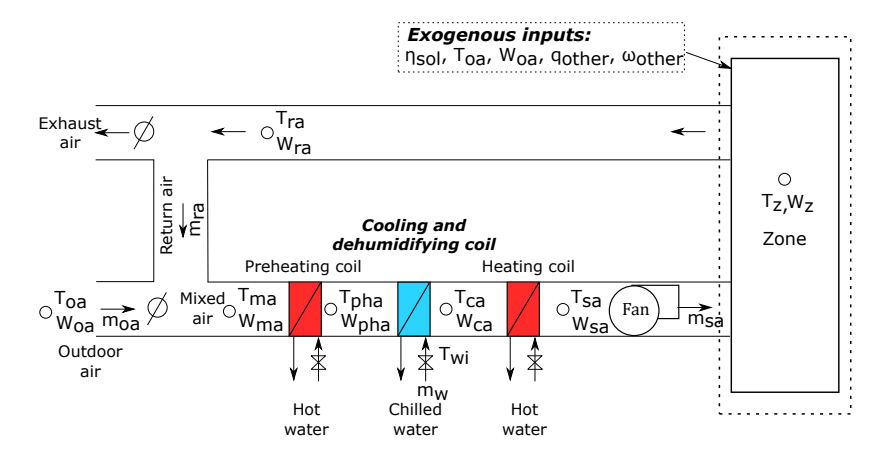


Figure 2: Schematic of a single-zone commercial variable-air-volume HVAC system. In this figure, oa: outdoor air, ra: return air, ma: mixed air, pha: preheated air, ca: conditioned air, and sa: supply air.

The role of a climate control system is to maintain thermal comfort and indoor air quality by varying the following control commands: (i) supply air flow rate (m_{sa}) , (ii) outdoor air ratio $(r_{oa} := \frac{m_{oa}}{m_{sg}} = \frac{m_{oa}}{m_{og} + m_{ra}})$, where m_{oa} and m_{ra} are the outdoor and return airflow rates respectively), (iii) conditioned air temperature (T_{ca}) , (iv) supply air temperature (T_{sa}) , and (v) preheated air temperature (T_{pha}) . So the control command vector is:

$$u := [m_{sa}, r_{oa}, T_{ca}, T_{sa}, T_{pha}]^T \in \mathfrak{R}^5$$
(1)

These five control commands are sent as set points to the low level control loops which are typically comprised of proportional-integral (PI) controllers.

The overall plant model consists of hygro-thermal dynamics of a single-zone building coupled with a cooling coil, heating coil, and a preheating coil. It is of the form $x_{k+1} = f(x_k, u_k, w_k)$ where x is the state vector, u is the input vector, and w is the exogenous input (disturbance) vector. The state vector consists of zone temperature (T_z) , wall temperature (T_w) , zone humidity ratio (W_z) , and conditioned air humidity ratio (W_{ca}) , i.e., $x := [T_z, T_w, W_z, W_{ca}]^T \in \mathfrak{R}^4$. The input vector is defined in (1). The exogenous input vector consists of solar irradiance (η_{sol}) , outdoor air temperature (T_{oa}) , outdoor air humidity ratio (W_{oa}) , internal heat load (q_{other}) due to occupants, lights, equipments, etc., and rate of internal water vapor generation (ω_{other}) due to occupants, equipments, etc. Therefore, $w := [\eta_{sol}, T_{oa}, W_{oa}, q_{other}, \omega_{other}]^T \in \mathfrak{R}^5$. The interested readers are referred to our prior work (Raman et al., 2020) for a detailed description of the mathematical models used for simulating the plant.

3. CONTROL ALGORITHMS

In this section, we describe three control algorithms: (i) the proposed MPC controller that incorporates humidity and latent heat (*SL-MPC*), (ii) an MPC controller that considers only sensible heat (*S-MPC*), and (iii) a rule-based controller for baseline (*BL*). All three controllers need to decide the same five control commands defined in (1).

The objective function that both MPC controllers try to minimize is the total energy consumption of the HVAC system over the planning horizon. For the HVAC system configuration presented in Figure 2, there are four main components which consume energy. They are fan, cooling coil, preheating coil, and reheating coil. We assume that the energy consumed by other components such as damper actuators is negligible. The total energy consumption of the HVAC system during time k is proportional to the total power at that time, which is:

$$P_{total}(k) := P_{fan}(k) + P_{cc}^{SL}(k) + P_{reheat}(k) + P_{preheat}(k),$$
(2)

where P_{fan} is the fan power consumption, P_{cc}^{SL} is the cooling coil power consumption, P_{reheat} is the reheating coil power consumption, and $P_{preheat}$ is the preheating coil power consumption. These are dependent on the supply air flow rate and the enthalpies of return air, outdoor air, preheated air, conditioned air, and supply air. The cooling coil power

consumption is given by:

$$P_{cc}^{SL}(k) := \frac{m_{sa}(k)[h_{pha}(k) - h_{ca}(k)]}{\eta_{cc}COP_c},$$
(3)

where h_{pha} and h_{ca} are the specific enthalpy of air before and after the cooling coil. Since we are using the enthalpy and not just the dry bulb temperature, the model accounts for both sensible and latent heat transfers, hence the superscript SL. The models for P_{fan} and P_{reheat} are the same as in (Raman et al., 2020). The only new addition is the preheating coil, whose power consumption is modeled as the heat it adds to the mixed air stream:

$$P_{preheat}(k) := \frac{m_{sa}(k)C_{pa}[T_{pha}(k) - T_{ma}(k)]}{\eta_{preheat}COP_h},$$
(4)

where T_{ma} is the mixed air temperature, $\eta_{preheat}$ is the efficiency of the preheating coil, and COP_h is the boiler coefficient of performance.

3.1 Proposed Model Predictive Controller Incorporating Humidity and Latent Heat (SL-MPC)

This controller is an extension of the MPC presented in our prior work (Raman et al., 2020). The optimization problem underlying the proposed MPC controller has the following decision variables: states of the process $x(k) := [T_z(k), W_z(k)]^T \in \mathfrak{R}^2$, the vector of control commands and internal variables $v(k) := [u(k)^T, m_{w,T}(k), m_{w,W}(k), W_{ca}(k)]^T \in \mathfrak{R}^8$, where u(k) is the control command vector defined in (1), and the vector of nonnegative slack variables $\zeta(k) := [\zeta_T^{low}(k), \zeta_T^{low}(k), \zeta_W^{low}(k), \zeta_W^{high}(k), \zeta_{m_w}(k-1)] \in \mathfrak{R}^5$ which is introduced for feasibility of the optimization problem. The exogenous input vector is defined as: $w(k) := [\eta_{sol}(k), T_{oa}(k), W_{oa}(k), q_{other}(k), \omega_{other}(k)]^T \in \mathfrak{R}^5$.

Mathematically the optimization problem at time index j is:

$$\min_{V,X,Z} \sum_{k=j}^{j+N-1} \left[P_{fan}(k) + P_{cc}^{SL}(k) + P_{reheat}(k) + \lambda_{preheat} P_{preheat}(k) \right] \Delta t + P_{slack}(k), \tag{5a}$$

where $V := [v^T(j), v^T(j+1), ..., v^T(j+N-1)]^T$, $X := [x^T(j+1), x^T(j+2), ..., x^T(j+N)]^T$, $Z := [\zeta^T(j+1), \zeta^T(j+2), ..., \zeta^T(j+N)]^T$, and time between j and j+1 is Δt . The last term, P_{slack} , penalizes the zone temperature, zone humidity, and chilled water flow rate slack variables:

$$P_{slack}(k) \coloneqq \lambda_T^{low} \zeta_T^{low}(k+1) + \lambda_T^{high} \zeta_T^{high}(k+1) + \lambda_W^{low} \zeta_W^{low}(k+1) + \lambda_W^{high} \zeta_W^{high}(k+1) + \lambda_{m_w} \zeta_{m_w}(k),$$

where the λ s are penalty parameters. The optimal control commands are obtained by solving the optimization problem (5a) subject to the following constraints:

$$T_{z}(k+1) = T_{z}(k) + \frac{\Delta t}{C} \left[\frac{(T_{oa}(k) - T_{z}(k))}{R} + m_{sa}(k)C_{pa}(T_{sa}(k) - T_{z}(k)) + A_{e}\eta_{sol}(k) + q_{other}(k) \right]$$
(5b)

$$W_{z}(k+1) = W_{z}(k) + \frac{\Delta t R_{g} T_{z}(k)}{V P^{da}} \left[\omega_{other}(k) + m_{sa}(k) \frac{W_{sa}(k) - W_{z}(k)}{1 + W_{sa}(k)} \right]$$
 (5c)

$$T_{ca}(k) = T_{pha}(k) + m_{w,T}(k) f(T_{pha}(k), W_{pha}(k), m_{sa}(k), m_{w,T}(k))$$
(5d)

$$W_{ca}(k) = W_{pha}(k) + m_{w,W}(k) g(T_{pha}(k), W_{pha}(k), m_{sa}(k), m_{w,W}(k))$$
(5e)

$$m_{w,W}(k) = m_{w,T}(k) - \zeta_{m_w}(k) \tag{5f}$$

$$T_z^{low}(k) - \zeta_T^{low}(k) \le T_z(k) \le T_z^{high}(k) + \zeta_T^{high}(k) \tag{5g}$$

$$a^{low}T_z(k) + b^{low} - \zeta_W^{low}(k) \le W_z(k) \le a^{high}T_z(k) + b^{high} + \zeta_W^{high}(k)$$
(5h)

$$\max\left(m_{sa}(k) - m_{sa}^{rate}\Delta t, m_{sa}^{low}\right) \le m_{sa}(k+1) \le \min\left(m_{sa}(k) + m_{sa}^{rate}\Delta t, m_{sa}^{high}\right) \tag{5i}$$

$$\max \left(T_{pha}(k) - T_{pha}^{rate}\Delta t, T_{pha}^{low}, T_{ma}(k+1)\right) \le T_{pha}(k+1) \le \min \left(T_{pha}(k) + T_{pha}^{rate}\Delta t, T_{pha}^{high}\right) \tag{5j}$$

$$\max\left(r_{oa}(k) - r_{oa}^{rate}\Delta t, r_{oa}^{low}\right) \le r_{oa}(k+1) \le \min\left(r_{oa}(k) + r_{oa}^{rate}\Delta t, r_{oa}^{high}\right) \tag{5k}$$

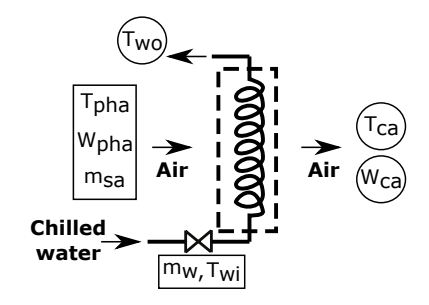


Figure 3: Schematic of a cooling coil.

$$\max\left(T_{ca}(k) - T_{ca}^{rate}\Delta t, T_{ca}^{low}\right) \le T_{ca}(k+1) \le \min\left(T_{ca}(k) + T_{ca}^{rate}\Delta t, T_{pha}(k+1)\right) \tag{51}$$

$$\max\left(T_{sa}(k) - T_{sa}^{rate}\Delta t, T_{ca}(k+1)\right) \le T_{sa}(k+1) \le \min\left(T_{sa}(k) + T_{sa}^{rate}\Delta t, T_{sa}^{high}\right) \tag{5m}$$

$$W_{ca}(k) \le W_{pha}(k) \tag{5n}$$

$$\zeta_T^{low}(k+1), \ \zeta_T^{high}(k+1) \ge 0 \tag{50}$$

$$\zeta_W^{low}(k+1), \ \zeta_W^{high}(k+1), \ \zeta_{m_w}(k) \ge 0 \tag{5p}$$

where constraints (5b)-(5f) and (5n)-(5p) are for k = j, ..., j + N - 1, constraints (5g) and (5h) are for k = j + 1, ..., j + N, and constraints (5i)-(5m) are for k = j - 1, ..., j + N - 2.

Constraints (5b) and (5c) are for the discretized temperature and humidity dynamics model of the zone respectively. Constraints (5d)-(5f) are for the control-oriented cooling coil model and is presented in the next subsection (Section 3.1.1). Constraints (5g) and (5h) are box constraints to maintain temperature and humidity of the zone within the allowed comfort limits. Usually the limits during the unoccupied mode are more relaxed than the occupied mode, i.e., $[T_z^{low,occ}, T_z^{high,occ}] \subseteq [T_z^{low,unocc}, T_z^{high,unocc}]$ and $[RH_z^{low,occ}, RH_z^{high,occ}] \subseteq [RH_z^{low,unocc}, RH_z^{high,unocc}]$, where RH_z is the relative humidity of the zone. RH_z is a highly nonlinear function of dry bulb temperature and humidity ratio (ASHRAE, 2017, Chapter 1). We linearize this function which gives us the coefficients a^{low} , b^{low} , a^{high} , and b^{high} in (5h), and helps in converting the constraints on relative humidity to humidity ratio.

Constraint (5i) is to take into account the capabilities of the fan. The minimum supply airflow rate is computed based on the ventilation requirements specified by ASHRAE 62.1 (ASHRAE, 2016) and to maintain positive building pressurization

Constraints (5j)-(5m) are to take into account the capabilities of the preheating coil, damper actuators, cooling coil, and reheating coil. In constraints (5j) and (5m), the inequalities $T_{pha}(k+1) \ge T_{ma}(k+1)$ and $T_{sa}(k+1) \ge T_{ca}(k+1)$ ensure that the preheating and reheating coils can only add heat; it cannot cool. Similarly, in constraints (5l) and (5n), the inequalities $T_{ca}(k+1) \le T_{pha}(k+1)$ and $W_{ca}(k) \le W_{pha}(k)$ ensure that the cooling coil can only cool and dehumidify the air stream; it cannot add heat or moisture. Inequality constraints (5o) and (5p) ensure that the slack variables are nonnegative.

3.1.1 Control-oriented cooling coil model: Constraints (5d), (5e), and (5f) are for the control-oriented cooling coil model, which is a modified version of the model developed in (Raman et al., 2020). Figure 3 shows the schematic of a cooling coil. The inputs to the model are supply air flow rate (m_{sa}) , chilled water flow rate (m_w) , inlet water temperature $(T_{w,i})$, and temperature (T_{pha}) and humidity ratio (W_{pha}) of the air before the coil. The outputs are conditioned air temperature (T_{ca}) and humidity ratio (W_{ca}) .

First we describe the reduced-order model proposed in (Raman et al., 2020), before discussing the modifications needed to make the MPC formulation climate/weather independent. It is a static model with the outputs being a polynomial function of the inputs. Note that when the chilled water flow rate is zero, no cooling or dehumidification of the air occurs. In that situation, the temperature and humidity ratio of the air before and after the coil must be equal: $T_{ca} = T_{pha}$

and $W_{ca} = W_{pha}$, when $m_w = 0$. To make the model have this behavior, the following functional form is chosen:

$$T_{ca}(k) = T_{pha}(k) + m_w(k) f(T_{pha}(k), W_{pha}(k), m_{sa}(k), m_w(k))$$
(6)

$$W_{ca}(k) = W_{pha}(k) + m_w(k) g(T_{pha}(k), W_{pha}(k), m_{sa}(k), m_w(k))$$
(7)

where functions f and g are chosen as quadratic in their arguments.

Now we discuss the modifications proposed here, which are needed to make the MPC formulation climate/weather independent. In hot-dry weather conditions, the cooling coil might be providing only cooling without any dehumidif-cation. In such a situation, the temperature of the air after the coil will be cooler than the air before the coil, while the humidity of the air before and after the coil will be the same, i.e., $T_{ca} < T_{pha}$ and $W_{ca} = W_{pha}$. For the model to have this behavior, we split the chilled water flow rate m_w into two virtual variables $m_{w,T}$ and $m_{w,W}$ as shown below:

$$T_{ca}(k) = T_{pha}(k) + m_{w,T}(k) f(T_{pha}(k), W_{pha}(k), m_{sa}(k), m_{w,T}(k))$$
(8)

$$W_{ca}(k) = W_{pha}(k) + m_{w,W}(k) g(T_{pha}(k), W_{pha}(k), m_{sa}(k), m_{w,W}(k)).$$
(9)

We also introduce the equality constraint (5f): $m_{w,W}(k) = m_{w,T}(k) - \zeta_{m_w}(k)$, where $\zeta_{m_w}(k)$ is a non-negative slack variable which is penalized in the objective function (5a). The main idea behind these modifications is that, inequality constraint (5n): $W_{ca}(k) \leq W_{pha}(k)$, will be active in hot-dry weather conditions, forcing $m_{w,W}(k)$ to be zero while $m_{w,T}(k)$ can be non-zero. This allows for cooling without any dehumidification, i.e., $T_{ca} < T_{pha}$ and $W_{ca} = W_{pha}$, as $m_{w,T} \neq 0$ while $m_{w,W} = 0$. The high penalty on the slack variable (ζ_{m_w}) ensures that the two chilled water flow rate variables are equal most of the time and is used only under extreme conditions when the model is not able to predict well. In Section 5.3 we discuss how these design choices helped the controller to perform well under various conditions.

3.2 Model Predictive Controller Incorporating Only Sensible Heat (S-MPC)

This controller is similar to the one described in Section 3.1, with the main difference being that the moisture and latent heat of air are not considered. The optimization problem formulation is similar to the one presented in (Ma et al., 2012).

There are five main differences when compared to SL-MPC: (i) The cooling power term in the objective function is based only on sensible heat; latent heat is ignored. (ii) S-MPC does not need zone humidity measurement. (iii) Since S-MPC does not consider humidity and latent heat, the constraints placed on the humidity at various locations in the air loop as well as the zone—(5c), (5h), (5n), and (5p)—are no longer used. (iv) The constraints placed on the system due to the cooling and dehumidifying coil model—(5d), (5e), and (5f)—are also not present. (v) Prediction of the exogenous inputs W_{oa} and ω_{other} which are used to compute humidity related constraints, are not needed. The interested readers are referred to the S-MPC controller presented in (Raman et al., 2020, Section 3.2) for details.

3.3 Baseline Controller (BL)

The rule-based *Dual Maximum* (ASHRAE, 2011) controller is used as the baseline controller. Even though the *Single Maximum* controller is widely used, the *Dual Maximum* controller is more energy-efficient among the two (ASHRAE, 2011; Goyal et al., 2013). The *Dual Maximum* controller operates in three modes based on the zone temperature: (i) Cooling, (ii) Deadband, and (iii) Heating. The supply airflow rate (m_{sa}) and temperature (T_{sa}) are varied based on the mode. The conditioned air temperature (T_{ca}) is typically at a low value $(12.8^{\circ}C)$, which ensures that air supplied to the zone is sufficiently dry at all times (Williams, 2013). The outdoor air ratio (r_{oa}) is varied to maintain the ventilation requirements dictated by ASHRAE 62.1 (ASHRAE, 2016) and positive building pressurization requirements. If the mixed air temperature is too cold, then the preheated air temperature (T_{pha}) is maintained typically at $12.8^{\circ}C$ ($55^{\circ}F$), which protects the cooling coil from freezing. Details of the *Dual Maximum* controller can be found in (ASHRAE, 2011).

4. SIMULATION SETUP

4.1 Plant Parameters

The plant simulation parameters are chosen based on a large classroom/auditorium (~ 6 m high and floor area of ~ 465 m²) in Pugh Hall located at the University of Florida, USA. We present only the relevant details here, the interested readers are referred to (Raman et al., 2020) for a complete list of the parameter values used.

The scheduled occupancy is from 7:30 AM to 7:00 PM, Monday to Friday, during which the following constraints are used: $T_z^{low,occ} = 21.1^{\circ}C$ ($70^{\circ}F$), $T_z^{high,occ} = 23.3^{\circ}C$ ($74^{\circ}F$), $RH_z^{low,occ} = 10\%$, and $RH_z^{high,occ} = 60\%$. The unoccupied hours are from 7:00 PM to 7:30 AM, Monday to Friday, and all of Saturday and Sunday, during which the following constraints are used: $T_z^{low,unocc} = 18.9^{\circ}C$ ($66^{\circ}F$), $T_z^{high,unocc} = 25.6^{\circ}C$ ($78^{\circ}F$), $RH_z^{low,unocc} = 10\%$, and $RH_z^{high,unocc} = 60\%$.

We assume that during weekdays there are 175 people present in the building between 7:30 AM to 11:30 AM and 12:30 PM to 7:00 PM. q_{other} and ω_{other} are computed based on the number of occupants (n_p) in the zone, assuming that each person produces 100 W of heat and 1.39×10^{-5} kg/s (50 g/h) of water vapor (ASHRAE, 2017). For q_{other} , an additional heat load of 6000 W is considered based on lighting/equipment power density of 12.92 W/m² (1.2 W/ft²), during the scheduled occupancy. This additional heat load is reduced to 3000 W during the unoccupied hours.

4.2 Controller Parameters

MPC parameters: The optimization problem is solved using CasADi (Andersson et al., 2019) and IPOPT (Wächter & Biegler, 2006), a nonlinear programming (NLP) solver, on a Desktop Linux computer with 16GB RAM and a 3.60 GHZ \times 8 CPU. We use a time step of $\Delta t = 10$ minutes and prediction/planning horizon N = 144 (corresponding to 24 hours). Therefore, there are 2160 (=144 \times {2+8+5}) decision variables for *SL-MPC*, and there are 1152 (=144 \times {1+5+2}) decision variables for *S-MPC*. On an average, the optimization problem in *SL-MPC* takes 7 seconds to solve, while the optimization problem in *S-MPC* takes 1.5 seconds to solve.

The MPC controllers require prediction of exogenous inputs. We compute the loads due to occupants in q_{other} and ω_{other} by assuming designed number of occupants (175) during the scheduled hours of occupancy. The remaining exogenous inputs are assumed to be fully known.

We assume that the number of occupants in the zone is not measured. So the MPC controllers need to ensure that the outdoor air needed to satisfy the ventilation requirements corresponding to the designed number of occupants (175), is provided during the scheduled hours of occupancy, according to ASHRAE 62.1 (ASHRAE, 2016).

For *SL-MPC*, the coefficients for the humidity constraint in (5h) are $a^{high} = 0.000621 \ kg_w/kg_{da}/^{o}C$, $b^{high} = -0.173323 \ kg_w/kg_{da}$, $a^{low} = 0.000101 \ kg_w/kg_{da}/^{o}C$, and $b^{low} = -0.028104 \ kg_w/kg_{da}$.

4.3 Performance Metrics

We use three performance metrics to compare the controllers: (i) the total energy consumed for a week (E_{total}), (ii) integral of the zone temperature violation for a week (V_T), and (iii) integral of the zone humidity violation for a week (V_{RH}). These are the same as defined in (Raman et al., 2020, Section 4.3) with three key differences: (i) the total energy consumed includes the preheating coil as well, (ii) for the humidity violation, we use relative humidity instead of humidity ratio, and (iii) the metrics are computed for a week (168 hours) instead of a day.

5. RESULTS AND DISCUSSIONS

We compare the performance of the three controllers in simulations by using weather data from two different locations: (i) Miami in Florida, which is considered to be "hot-humid" and belongs to climate zone 1A according to the International Energy Conservation Code (International Code Council, Inc., 2018), and (ii) Tucson in Arizona, which is considered to be "hot-dry" and belongs to climate zone 2B (International Code Council, Inc., 2018). The weather data for these locations are obtained from the National Solar Radiation Database (nsrdb.nrel.gov).

For both the locations, four one-week simulations are performed by choosing weather data from different seasons: spring, summer, fall, and winter. Figure 4a shows the total energy consumed when using the three controllers for different climate zones and seasons. Figure 4b shows the corresponding humidity violation. The temperature violation was found to be negligible for all the three controllers and therefore is not presented. The simulation results indicate the following:

- The proposed unified *SL-MPC* formulation performs well in both climate zones and in all the seasons; refer to Section 5.3 to see how our design choices helped the controller to perform well under various conditions.
- *SL-MPC* consumes the least amount of energy when compared to *BL*. The energy savings is up to 27% depending on the climate zone and season. We remark here that the baseline controller used for comparison is the energy-efficient *Dual Maximum*.

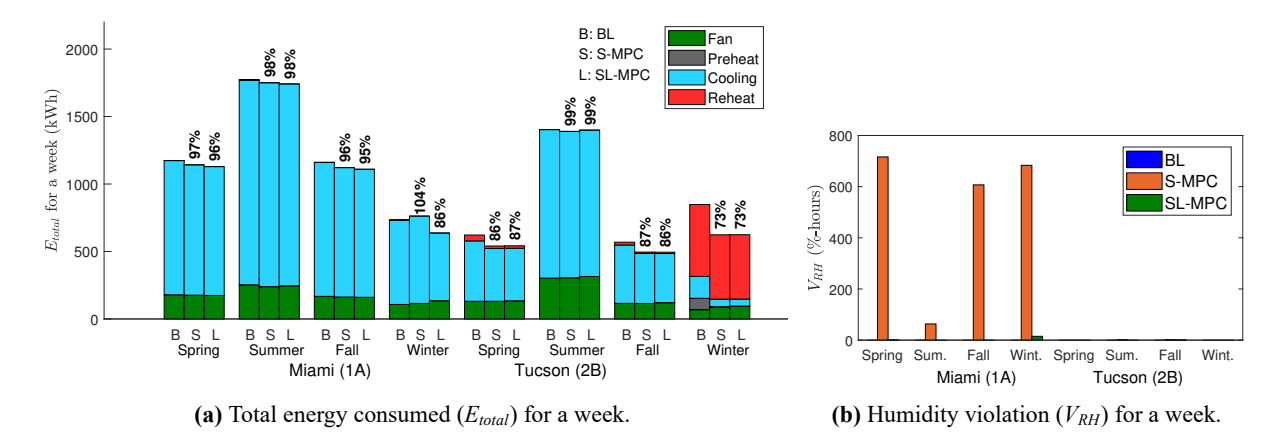


Figure 4: Performance comparison of *SL-MPC* (proposed controller), *S-MPC*, and *BL* for different climate zones and seasons.

- Moreover, using *SL-MPC* leads to negligible violation in temperature and humidity constraints under all conditions.
- S-MPC leads to large humidity violations in Miami.
- In addition to the humidity violations in Miami, S-MPC also consumes much more energy (17%) when compared to SL-MPC.
- The control decisions made by SL-MPC and S-MPC are found to be similar in Tucson.

These results are discussed in detail next.

5.1 Miami: Climate Zone 1A

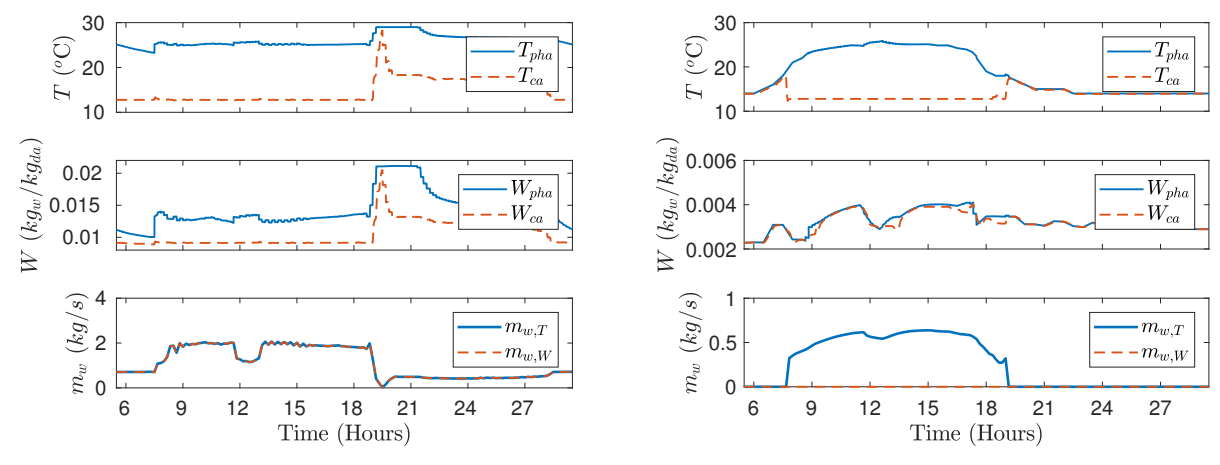
Using SL-MPC leads to significant energy savings (14%) mainly during winter when compared to BL. There are two main reasons for energy savings by SL-MPC. One, SL-MPC varies the conditioned air temperature (T_{ca}) as long as the humidity constraints are not violated and the cooling load in the zone is met. On the other hand, BL keeps T_{ca} at a constant low value of $12.8^{\circ}C$ (55°F) in the interest of maintaining indoor humidity, which leads to higher cooling energy consumption. Two, SL-MPC varies the outdoor air ratio and supply air flow rate to use as much "free cooling" as possible when the outdoor weather is mild and dry. While, BL brings in only the minimum outdoor air needed to satisfy the ventilation and building pressurization requirements. During summer, spring, and fall, the outdoor weather is pretty warm and humid, so the room for optimization and, thus, energy savings is less.

Using S-MPC leads to large humidity violations in spring, fall, and winter; see Figure 4b. It tries to use free cooling, mainly during nighttime, as the outdoor air is cooler than the return air. But the outdoor air is humid, which it is unaware of. In an attempt to reduce the cooling energy used further, it varies T_{ca} . Both these factors lead to humid air being supplied to the zone leading to indoor humidity violations. During summer the cooling load of the zone is high, so S-MPC decides to keep T_{ca} low which has an unintended, but good, side effect of maintaining indoor humidity. For SL-MPC, the humidity constraints are explicitly imposed, thus, it varies the control inputs in a way that no violations occur; see Figure 4b. Even in the case of BL there are no humidity violations because of the conservatively designed set point for T_{ca} (12.8°C).

Using S-MPC also leads to higher energy use than both BL and SL-MPC in winter; see Figure 4a. This is because it tries to use free cooling without realizing that the outdoor air is cool but humid. This leads to a higher latent load on the cooling coil and, thus, higher cooling energy consumption.

5.2 Tucson: Climate Zone 2B

Using *SL-MPC* leads to significant energy savings (13% to 27%) when compared to *BL* mainly during spring, fall, and winter. This is because of the same reasons mentioned in Section 5.1. In addition to these, *SL-MPC* avoids preheating completely during winter by recirculating as much warm air from the zone as possible. It satisfies the outdoor air



- (a) Summer in Miami: both cooling $(T_{ca} < T_{pha})$ and dehumidification $(W_{ca} < W_{pha})$ are seen to occur as the weather is hot and humid.
- **(b)** Spring in Tucson: there is cooling $(T_{ca} \le T_{pha})$ but no dehumidification $(W_{ca} = W_{pha})$ as the weather is hot and dry.

Figure 5: Simulations for a day using SL-MPC, showing that it works well in both humid and dry weather conditions. Top to bottom: temperature before (T_{pha}) and after (T_{ca}) the cooling coil, humidity ratio before (W_{pha}) and after the cooling (W_{ca}) coil, and chilled water flow rate $(m_{w,T})$ used by SL-MPC in constraint (5d) and chilled water flow rate $(m_{w,W})$ used by SL-MPC in constraint (5e).

requirements (m_{oa}) using a lower outdoor air ratio (r_{oa}) and a higher supply airflow rate (m_{sa}) . Whereas, BL is in the heating mode because of the cold weather in winter, so it uses a lower m_{sa} and thus a higher r_{oa} (recall that BL varies r_{oa} to maintain the minimum outdoor air requirements) to satisfy the same m_{oa} requirements. The usage of higher m_{sa} by SL-MPC leads to a slightly higher fan energy consumption but a substantial decrease in the preheating energy consumption; see the results for Tucson during winter in Figure 4a.

The decisions made by both the MPC controllers are found to be similar in Tucson; see Figure 4. This can be attributed to the dry outdoor weather in Tucson.

5.3 Autonomy of SL-MPC

The results and discussions presented in Sections 5.1 and 5.2 make it clear that the proposed *SL-MPC* controller works well in both humid and dry climate zones, and in all four seasons. In this section, we will be looking at how the design choices made in the MPC formulation helped the controller in performing well under various conditions.

Figure 5 shows the simulation results when using SL-MPC for a day in Miami and Tucson. It can be seen from Figure 5a that there is both cooling and dehumidification occurring in Miami as the outdoor weather is hot and humid. Moreover, the slack variable corresponding to the chilled water flow rate (ζ_{m_w}) is found to be 0 as $m_{w,T} = m_{w,W}$. However, in Tucson $\zeta_{m_w} \neq 0$, as $m_{w,T} \neq m_{w,W}$; see between 9:00-18:00 hrs in Figure 5b. Specifically $m_{w,W} = 0$ while $m_{w,T} \neq 0$, which allows for cooling without any dehumidification as the outdoor weather is hot and dry in Tucson. Such behaviors are made possible because of the following design choices: (i) the functional form of the control-oriented cooling coil model in (5d) and (5e), (ii) separating the chilled water flow rate into two virtual variables ($m_{w,T}$ and $m_{w,W}$), (iii) equality constraint (5f) with slack variable ζ_{m_w} and the heavy penalty on the slack variable in the objective function (5a), which ensures that the flow rates are different only when needed.

6. CONCLUSION

In our recent work (Raman et al., 2020) we showed the importance of inclusion of humidity and latent heat in an MPC formulation for energy-efficient HVAC control, especially in hot-humid climates. We showed that a humidity-agnostic MPC formulation can lead to poor humidity control, or higher energy usage as it is unaware of the latent load on the cooling coil. The MPC formulation that we had proposed in our prior work uses a reduced order cooling coil model which puts a limitation on its prediction accuracy in extreme climatic/weather conditions. In this work we present a

computationally tractable reformulation which addresses that limitation. Simulation results show that the unified MPC formulation proposed here performs better than a rule-based baseline controller in multiple climate zones and weather conditions.

REFERENCES

- Andersson, J. A. E., Gillis, J., Horn, G., Rawlings, J. B., & Diehl, M. (2019, Mar 01). Casadi: a software framework for nonlinear optimization and optimal control. *Mathematical Programming Computation*, 11(1), 1–36.
- ASHRAE. (2011). The ASHRAE handbook: HVAC applications (SI Edition).
- ASHRAE. (2016). ANSI/ASHRAE standard 62.1-2016, ventilation for acceptable air quality.
- ASHRAE. (2017). The ASHRAE handbook fundamentals (SI Edition).
- Goyal, S., Ingley, H., & Barooah, P. (2013, June). Occupancy-based zone climate control for energy efficient buildings: Complexity vs. performance. *Applied Energy*, 106, 209-221.
- International Code Council, Inc. (2018). International Energy Conservation Code.
- Kraemer, K., & Marquardt, W. (2010). Continuous reformulation of MINLP problems. In M. Diehl, F. Glineur, E. Jarlebring, & W. Michiels (Eds.), *Recent advances in optimization and its applications in engineering* (pp. 83–92). Springer.
- Ma, Y., Richter, S., & Borrelli, F. (2012, March). Chapter 14: Distributed model predictive control for building temperature regulation. *In Control and Optimization with Differential-Algebraic Constraints*, 22, 293-314.
- Raman, N. S., Devaprasad, K., Chen, B., Ingley, H. A., & Barooah, P. (2020, December). Model predictive control for energy-efficient HVAC operation with humidity and latent heat considerations. *Applied Energy*, 279, 115765. doi: https://doi.org/10.1016/j.apenergy.2020.115765
- Serale, G., Fiorentini, M., Capozzoli, A., Bernardini, D., & Bemporad, A. (2018). Model predictive control (MPC) for enhancing building and HVAC system energy efficiency: Problem formulation, applications and opportunities. *Energies*, 11(3), 631.
- Shaikh, P. H., Nor, N. B. M., Nallagownden, P., Elamvazuthi, I., & Ibrahim, T. (2014). A review on optimized control systems for building energy and comfort management of smart sustainable buildings. *Renewable and Sustainable Energy Reviews*, *34*, 409 429.
- Wächter, A., & Biegler, L. T. (2006, Mar 01). On the implementation of an interior-point filter line-search algorithm for large-scale nonlinear programming. *Mathematical Programming*, 106(1), 25–57.
- Williams, J. (2013). Why is the supply air temperature 55F? http://8760engineeringblog.blogspot.com/ 2013/02/why-is-supply-air-temperature-55f.html. (Last accessed: Aug. 03, 2020)

ACKNOWLEDGMENT

The research reported here has been partially supported by an NSF grant (award no. 1934322, CMMI) and the State of Florida through a REET (Renewable Energy and Energy Efficient Technologies) grant.